JOURNAL OF VIROLOGY, Oct. 1993, p. 6033–6046
0022-538X/93/106033-14$02.00/0

Vol. 67, No. 10

BCR-ABL and v-*abl* Oncogenes Induce Distinct Patterns of Thymic Lymphoma Involving Different Lymphocyte Subsets

STEVEN S. CLARK,[1,2]* ERIC CHEN,[1,2,3] MARCO FIZZOTTI,[1,2]† OWEN N. WITTE,[4,5] AND VERA MALKOVSKA[6]

Department of Human Oncology,[1] Comprehensive Cancer Center,[2] Medical Scientist Training Program and Human Cancer Biology Training Program,[3] and Department of Medicine, School of Medicine,[6] University of Wisconsin, Madison, Wisconsin 53792, and Department of Microbiology and Molecular Genetics[4] and Howard Hughes Medical Institute,[5] University of California, Los Angeles, California 90024

Received 18 March 1993/Accepted 29 June 1993

The human *BCR-ABL* oncogenes encoded by the Philadelphia chromosome (Ph) affect the pathogenesis of diverse types of leukemia and yet are rarely associated with T-lymphoid leukemia. To determine whether *BCR-ABL* kinases are inefficient in transforming T lymphocytes, *BCR-ABL*-expressing retroviruses were injected intrathymically into mice. Thymomas that expressed *BCR-ABL* kinase developed after a relatively long latent period. In most thymomas, deletion of 3′ proviral sequences resulted in loss of *tk-neo* and occasionally caused expression of kinase-active carboxy-terminally truncated *BCR-ABL* oncoprotein. In contrast, deletion of 3′ proviral sequences was not observed in thymomas induced with Abelson murine leukemia virus (A-MuLV). *BCR-ABL* viruses induced distinct patterns of disease and involved different thymocyte subsets than A-MuLV and Moloney murine leukemia virus (Mo-MuLV). While Mo-MuLV only induced Thy-1$^+$ thymomas, v-*abl*- and *BCR-ABL*-induced thymomas often contained mixed populations of B220$^+$ and Thy-1$^+$ lymphocytes in the same tumor. In most v-*abl* and *BCR-ABL* tumors, Thy-1$^+$ lymphoid cells expressed CD8 and a continuum of CD4 ranging from negative to positive. Conversely, Mo-MuLV thymomas contained distinct populations of CD4$^+$ cells that were either CD8$^+$ or CD8$^-$. A-MuLV-transformed T-lymphoid cells did not express the CD3/T-cell receptor complex, while *BCR-ABL* tumors were CD3$^+$. Thus, *BCR-ABL* viruses preferentially induce somewhat more differentiated T lymphocytes than are transformed by A-MuLV. Furthermore, rare B220$^+$ lymphocytes may represent preferred v-*abl* and *BCR-ABL* transformation targets in the thymus.

The v-*abl* oncogene of the Abelson murine leukemia virus (A-MuLV) encodes a 160-kDa *gag-abl* fusion protein with potent tyrosine kinase activity which can efficiently transform fibroblasts as well as cells of multiple hematopoietic lineages and maturational stages (reviewed in reference 52). However, the v-*abl* kinase usually induces acute transformation of early B lymphocytes, which has made it a valuable tool for characterizing immature stages of B-cell development. In humans, the *ABL* proto-oncogene is activated as a consequence of the t(9;22) Philadelphia chromosome translocation (Ph), which appends the *ABL* gene on chromosome 9 to different portions of the *BCR* gene on chromosome 22. This results in expression of either the P210 or P185 tyrosine kinase-active *BCR-ABL* fusion protein (reviewed in reference 9). Because the Ph translocation often arises in pluripotent bone marrow stem cells, *BCR-ABL* oncogenes are associated with the pathogenesis of many types of leukemia. Retrovirus-mediated gene transfer and transgenic mouse models have confirmed that *BCR-ABL* kinases can alter growth and differentiation in different immature hematopoietic cell types (17, 20, 21, 24, 27, 40). However, unlike the acute oncogenicity and arrested development of hematolymphoid cells transformed by v-*abl*, *BCR-ABL* transformants are poorly oncogenic and often are able to undergo significant differentiation (24, 55). Transformation with *BCR-ABL* oncogenes therefore represents an improvement over the v-*abl* transformation model for studying the signals that regulate growth versus differentiation in hematolymphoid precursor cells.

Under certain circumstances, A-MuLV can acutely transform immature T lymphocytes that are usually arrested in their development. This raises the possibility that transformation of thymocytes with *BCR-ABL* may be a useful approach for stimulating growth of T-lymphocyte precursors that retain significant developmental potential. However, studies with both humans and mice show that *BCR-ABL*-induced T-cell leukemia is extremely rare even when *BCR-ABL* is expressed in T lymphocytes (33) or in multipotential stem cells (17, 19, 29, 35, 57). T lymphocytes may therefore be poor transformation targets for *BCR-ABL*. In order to determine whether *BCR-ABL* oncogenes can efficiently transform early T lymphocytes, we injected *BCR-ABL*-expressing retroviruses into the thymi of young mice. This report compares the pathogenesis and phenotype of thymic lymphomas induced with P210- and P185-expressing viruses and of lymphomas induced by A-MuLV and Moloney murine leukemia virus (Mo-MuLV).

MATERIALS AND METHODS

Retroviruses. The construction of the P210 and P185 *BCR-ABL* retroviruses has been described (39, 40). Briefly, *BCR-ABL* cDNA copies containing 114 bp of 5′ *BCR* noncoding sequences were cloned into the *Eco*RI site of PMV6(tk-neo). This results in Mo-MuLV long terminal repeat (LTR)-driven expression of virus genome-length (9.5-kb) transcripts that carry *BCR-ABL* and *neo* coding se-

* Corresponding author.
† Present address: Clinica Medica I, Università di Perugia, Perugia, Italy.

quences (see diagram in Fig. 2). Mo-MuLV-rescued stocks of *BCR-ABL* and of Abelson viruses were collected from clonal NIH 3T3 fibroblast cells transformed with a helper-free defective virus and superinfected with Mo-MuLV. These were designated P210/M, P185/M, and A-MuLV/M.

Mo-MuLV levels in the different virus stocks were compared by slot blot hybridization analysis of serial dilutions of virion RNA with ecotropic *env* DNA and Mo-MuLV U3 LTR sequences as probes and by measuring reverse transcriptase activity, which has been shown to bear a linear relationship with the UV-XC plaque titer (45). According to both methods, the Mo-MuLV, P210/M, and P185/M viruses differed no more than 3-fold in the level of helper virus, while the A-MuLV/M stock had about 10-fold less helper virus.

The A-MuLV/M titer was 10^5 focus-forming units per ml, as measured on NIH 3T3 cells. Because *BCR-ABL* viruses do not efficiently transform fibroblasts, the levels of defective virus in the A-MuLV/M, P210/M, and P185/M stocks were first compared by viral RNA slot blot analysis of serial dilutions of virus stock with a probe for the conserved *ABL* kinase domain (41). The P210/M and A-MuLV/M stocks contained comparable levels of oncogene-expressing defective virus, while the P185 stock had fivefold less viral RNA. These results were confirmed by immunoblot analysis of *ABL* oncoprotein expression in acutely infected NIH 3T3 fibroblasts.

Tumor induction. Thymic lymphomas were induced by injecting 25 μl of virus supernatant containing 8 μg of Polybrene per ml into the surgically exposed thymic lobes of 5- to 6-week-old BALB/c mice. Sick animals were killed, and their spleens, thymi, livers, and lymph nodes (axillary and inguinal) were weighed. High-molecular-weight DNA and total RNA were prepared from lymphomas by standard procedures, and the remaining cells were cryopreserved for later analysis.

Protein and nucleic acid analyses. Immunokinase autophosphorylation analyses with site-specific anti-*ABL* and anti-*BCR* rabbit antisera were performed as described previously (5). Cell lysates were prepared for immunoblot analysis as reported by Muller et al. (42), and protein concentrations were determined by the bicinchoninic acid method (Pierce). Cellular proteins were fractionated by 7 to 8% polyacrylamide gel electrophoresis (PAGE) with sodium dodecyl sulfate (SDS) and transfered to nitrocellulose membranes. The blots were probed with monoclonal anti-*ABL* antibodies Ab2 and Ab3 (Oncogene Science) and then with horseradish peroxidase-conjugated protein A as described in the figure legends. The enhanced chemiluminescence method (Amersham) was used for detection.

DNA and RNA were analyzed by standard blotting procedures with probes labeled with [^{32}P]CTP by random oligonucleotide priming. Different autradiographic exposures were made so that relative band intensities could be compared by laser densitometry with a 2202 Ultroscan (LKB). A 1.8-kb chicken actin cDNA probe was provided by David Spriggs, University of Wisconsin–Madison. The *ABL* kinase domain probe was a 0.65-kb *Pst*I fragment from pJW-P4 (41), and the v-*abl* probe consisted of a 2-kb *Sac*I-*Hin*dIII fragment from pAB3Sub3 (25). 5′ *BCR* sequences were probed with a 3.5-kb *Eco*RI fragment from pK562-172 (41). *neo* sequences were detected with a 0.9-kb *Eco*RI-*Pst*I fragment from pSV2neo. For examining the immunoglobulin heavy-chain gene *IgH*, a 1.8-kb *Bam*HI-*Eco*RI genomic J_H region fragment was used (18). The T-cell receptor (TCR) gamma locus was examined with a murine Jγ1 probe, which cross-hybridizes to Jγ2 and Jγ3 (32). The 0.8-kb *Pst*I probe from pRBL-5 (28) used to examine the structure of the TCR Cβ1 gene does not cross-hybridize with Cβ2.

TABLE 1. Thymomagenesis by *BCR-ABL*

Virus	No. of mice	No. of diseased mice[a] (% of total)		Median latency period, days (range)	
		Onc$^+$	Onc$^-$	Onc$^+$	Onc$^-$
A-MuLV/M	21	13 (62)	2 (9)	32 (25–59)	79–80
P185/M	48	17 (35)	17 (35)	70 (51–108)	101 (51–120)
P210/M	57	18 (32)	9 (16)	80 (58–125)	113 (62–120)
Mo-MuLV	27		15 (55)		102 (81–157)

[a] Onc$^+$, tumors expressing kinase-active oncoproteins; Onc$^-$, tumors that do not express an *ABL* kinase but arise in mice injected with an oncogene-carrying virus.

Flow cytometry. Primary thymic lymphomas and normal control tissues were analyzed by one- and two-color flow cytometry after staining with phycoerythrin- and/or fluorescein isothiocyanate (FITC)-conjugated monoclonal antibodies specific for mouse B220, Thy-1, CD3, CD4, and CD8. Fluorochrome-conjugated antibodies (including isotype controls) were purchased from Pharmingen or Becton Dickinson. The majority of the dead cells present after cryopreserved samples were thawed were first removed by agglutination in high-phosphate buffer and further excluded from analysis by staining with propidium iodide.

RESULTS

***BCR-ABL* kinase expression correlates with distinct patterns of thymic lymphoma.** The ability of *BCR-ABL* oncogenes to transform immature T lymphocytes was tested by intrathymic injection of BALB/c mice with retroviruses that express P210 or P185 from *BCR-ABL* cDNA copies. Because these viruses are poorly oncogenic when inoculated into animals via several routes (23), we chose to inject thymi with Mo-MuLV-pseudotyped *BCR-ABL* viruses (P210/M and P185/M, respectively). While this approach increased the chance of infecting potentially rare thymocyte targets (31), it also raised the concern of whether it would be possible to distinguish the contribution of the weak *BCR-ABL* oncogenes from that of Mo-MuLV to the generation of malignancy. To investigate this, we compared the latency and pattern of disease that developed in animals injected with Mo-MuLV, P210/M, and P185/M. A-MuLV/M-injected animals were also included for comparison.

Table 1 summarizes the data on the latency of tumor formation. Mice injected with Mo-MuLV were slower to develop symptoms of disease (rough fur, lethargy, generalized lymphadenopathy, and splenomegaly) than animals injected with either P210/M or P185/M, which developed a distinct pattern of symptoms including cachexia, acute dyspnea, and occasional paraplegia. Neither the P210/M nor the P185/M virus caused tumors as rapidly as A-MuLV/M. P185-expressing thymomas arose somewhat faster than those expressing P210, which is consistent with previous reports that P185 is a more potent oncogene than P210 (40).

To compare the gross pathological patterns of disease induced by the different viruses, the weights of the thymus, spleen, and lymph nodes were measured after autopsy (Fig. 1, and data not shown). A-MuLV/M induced variable splenomegaly and thymoma, as reported previously (10), while mice inoculated intrathymically with Mo-MuLV characteristically developed mild to moderate thymic lymphoma

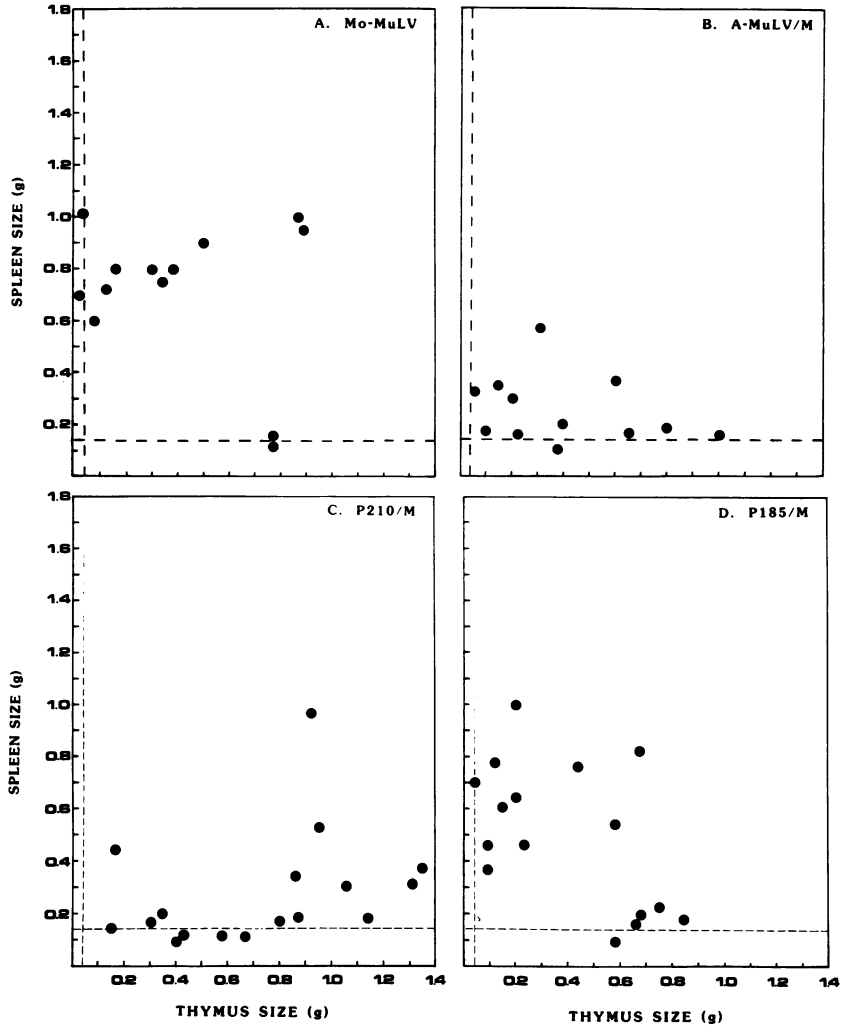

FIG. 1. Patterns of lymphoma induced by intrathymic injection of Mo-MuLV, A-MuLV/M, P210/M, and P185/M viruses. The pattern of disease was determined by measuring spleen and thymus weights after autopsy of moribund animals injected with the indicated virus. Dashed lines indicate normal weights for the spleen and thymus of mature female BALB/c mice.

with extensive peripheral lymphoma and hepatosplenomegaly. In contrast to these patterns of disease, P210 expression correlated with a moderate to large thymic lymphoma and only minimal peripheral involvement. Both the Mo-MuLV and the P210 patterns of disease were observed in animals whose tumors expressed P185, yet there were no obvious differences in oncogene expression or in the phenotype of the thymic lymphoma that could explain the development of distinct pathologies in these animals. It is possible that the Mo-MuLV helper virus exerts distinct effects on the pathogenesis of P185/M-induced tumors in different animals, but a similar effect on pathogenesis was not seen in animals whose tumors were induced with P210/M.

About 30 to 50% of the animals injected with P210/M or P185/M and 13% of those injected with A-MuLV/M developed thymic tumors which did not express kinase-active oncoprotein and were more similar to Mo-MuLV-injected animals in terms of tumor latency and pattern of disease (Table 1). Thymic tumors from these animals did carry proviral sequences that were detectable with an Mo-MuLV U3 LTR-specific probe but not with an *ABL*, *BCR*, or *neo* probe (data not shown). These observations indicate that tumors arising in mice without evidence of oncogene expression probably represent Mo-MuLV-induced thymomas. This correlation between oncogene expression and the distinct pattern and timing of lymphoma formation supports a role for *BCR-ABL* in the induction of thymic lymphoma.

In order to better understand the role of P210 and P185 in thymomagenesis, *BCR-ABL*-induced tumors were compared with Mo-MuLV- and A-MuLV-induced tumors with regard to oncogene expression, tumor clonality, and phenotype. P210- and P185-induced thymomas were similar by these analyses; therefore, the data presented focus on P210-induced tumors as representative of *BCR-ABL* thymomas.

***BCR-ABL* expression in thymic lymphomas is lower and more variable than v-*abl* expression.** Both immunoblot (Fig. 2A) and immunokinase analyses (data not shown) of primary thymomas showed that the *BCR-ABL* oncogene products were expressed at lower and more variable levels than those of v-*abl*. The relative level of P210 BCR-ABL expression was compared with the level of P160 v-*abl* expression by laser densitometry of different exposures of the immunoblot

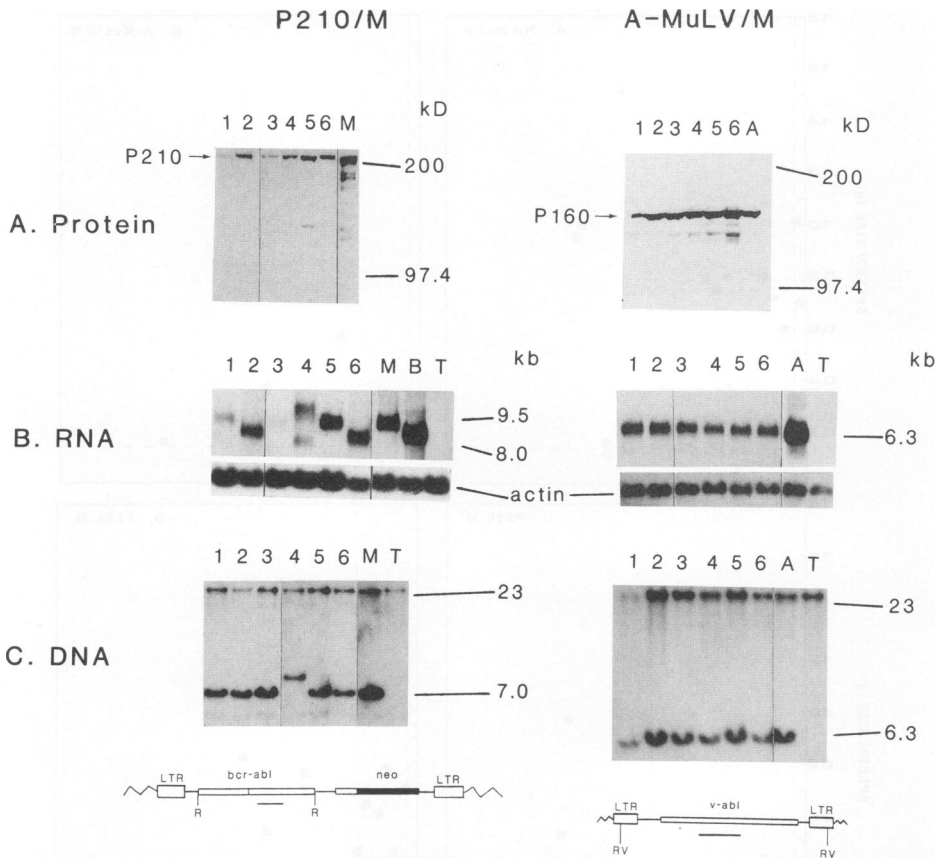

FIG. 2. Comparison of oncogene expression in primary thymic lymphomas transformed with P210/M and A-MuLV/M. (A) Immunoblot analysis of P210 *BCR-ABL* and P160 v-*abl* expression. Viably frozen tumor cells were thawed and immediately lysed in boiling SDS lysis buffer; 75 μg of protein was loaded into each lane and electrophoresed through an SDS–8% PAGE gel. Lysates from P210/M and A-MuLV/M tumors were run on the same gel and analyzed simultaneously. Blots were probed with anti-*ABL* monoclonal antibody Ab2, directed against the conserved kinase domain. With enhanced chemiluminescent detection, the exposure time was 30 min for P210 tumors and 5 min for A-MuLV tumors. A parallel gel was stained with Coomassie blue to ascertain even protein loading. (B) Analysis of proviral RNA expression by blot hybridization. Total RNA from each tumor (10 μg per lane) was fractionated on a 1% agarose–formaldehyde gel and transferred to Gene-Screen Plus (DuPont). RNA from P210/M tumors was probed with an *ABL* kinase domain probe, while RNA from A-MuLV tumors was probed with a fragment from PAB3SUB3. Filters were stripped and rehybridized with a chicken actin probe. Molecular size designations are published values, and the positions of the large and small rRNA subunits were visualized by ethidium bromide staining. (C) Structure of the integrated proviral oncogene. High-molecular-weight P210/M tumor DNA was digested with *Eco*RI (R) and A-MuLV/M tumor DNA was cut with *Eco*RV (RV), electrophoresed through 0.8% agarose, transferred to Gene-Screen Plus, and hybridized with the same probes used for the RNA analysis. Proviral restriction enzyme sites and the approximate positions of the hybridization probes are shown below the gels. Controls: lane M, M4 cells (P210 *BCR-ABL*-transformed pre-B cells) (39); lane B, 78B4 cells (P185 *BCR-ABL*-transformed pre-B cells) (40); lane A, A7 cells (P160 v-*abl*-transformed pre-B cells) (7); lane T, uninfected thymus cells. Laser densitometry was performed on lighter exposures in order to ensure that measurement was made in the linear exposure range of the X-OMAT AR film (Kodak).

shown in Fig. 2A. After correction for length of exposure, P210 was found to be expressed at approximately 5- to 20-fold-lower levels than P160. When normalized to actin RNA expression, *BCR-ABL* RNA expression was also found to be variable and correlated well with the level of steady-state retroviral RNA (compare Fig. 2A and B). In these blots, the normal murine c-*abl* protein and mRNA were not easily detected because of their low level of expression (39). Thus, relative to the levels of c-*abl* and v-*abl*, *BCR-ABL* oncogenes were detected at intermediate levels in the thymic lymphomas.

These and other data also showed that about 80% of the *BCR-ABL*-induced tumors but none of the v-*abl*-induced tumors expressed proviral RNA bands of unexpected length that were detectable with an internal *ABL* kinase domain probe (Fig. 2B) but not detectable with a 3′ *neo* probe (data not shown). In order to identify the basis for the variable structure and expression of *BCR-ABL* transcripts, genomic DNA from P210-induced thymomas was digested with *Eco*RI, which should resolve the P210 *BCR-ABL* coding region into a single 7.0-kb band detectable with a probe to the conserved kinase region. The relative contribution of *BCR-ABL*-transformed cells to the tumor population was measured by densitometry to compare the hybridization intensity of the proviral band with that of the germ line c-*abl* band as a control for DNA loading in each lane. The results demonstrated that the relative proviral DNA content did not vary more than twofold between individual *BCR-ABL* tumors (Fig. 2C). Thus, differences between tumors in the level of *BCR-ABL* expression did not appear to be due to the

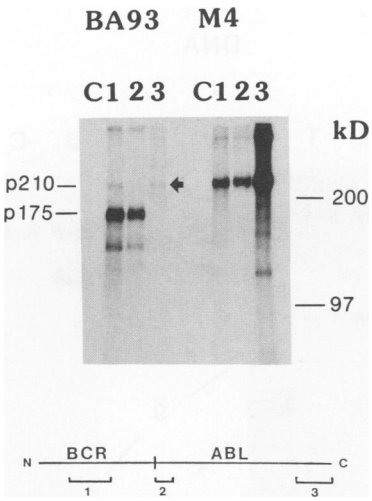

FIG. 3. Expression of kinase-active carboxy-terminally truncated P210 *BCR-ABL*. Cells from primary thymoma (BA9.3) or control M4 cells, which express full-length P210 from the P210 provirus (39), were lysed, immunoprecipitated, and processed for the autokinase reaction. Lane numbers correspond to the site-specific rabbit antiserum used for immunoprecipitation indicated in the lower panel (6). Lane C, preimmune rabbit serum. The arrow points to the faintly expressed full-length P210 protein that is precipitated with all three *BCR-ABL*-specific antisera.

efficiency of *BCR-ABL* retrovirus infection or to a variable contribution of Mo-MuLV-transformed cells to the tumor population.

Most P210-induced thymomas carried the expected 7.0-kb *BCR-ABL* restriction fragment, with the notable exception shown in lane 4 of Fig. 2C (left panel). DNA from this tumor also failed to hybridize to the *neo* probe, suggesting that recombination in 3′ proviral sequences resulted in the loss of *neo* sequences and the 3′ *Eco*RI site. Other *BCR-ABL* tumors that expressed aberrant proviral transcripts (Fig. 2B, lanes 2 and 6) often carried an apparently normal 7.0-kb *Eco*RI proviral DNA fragment detectable with the *ABL* kinase domain probe (Fig. 2C, lanes 2 and 6). However, these tumors also did not carry proviral DNA that hybridized to the *neo* probe (data not shown). Together, these results demonstrate that 3′ proviral recombination frequently results in loss of *neo* and may occasionally affect the *BCR-ABL* sequence. Similar structural abnormalities were not seen in the integrated v-*abl* genome or in the proviral message of A-MuLV-induced tumors (Fig. 2B and C, right panels). Thus, the lower and more variable expression of *BCR-ABL* RNA and protein may be due, in part, to loss of the 3′ proviral sequences such as the downstream LTR.

Some *BCR-ABL*-induced thymic lymphomas express truncated P210 or P185 kinase. Although the loss of 3′ proviral sequences usually did not appreciably affect the *BCR-ABL* coding region, 4 of 14 P210 thymomas and 1 of 13 P185 tumors expressed truncated *BCR-ABL* polypeptides. With a panel of *BCR-ABL* product site-specific antisera, all truncated proteins were shown to have lost *ABL* carboxy-terminal epitopes while retaining high-level kinase activity (Fig. 3 and data not shown). Full-length *BCR-ABL* kinase-active proteins could also be detected in these tumors, but at 5 to 20% of the level of the truncated kinase (Fig. 3 and 4A).

The basis for this pattern of *BCR-ABL* expression was investigated in three independent tumors that expressed truncated P210. Immunoblot analysis of *BCR-ABL* expression confirmed that truncated polypeptides were expressed at higher levels than the full-length proteins (Fig. 4A). RNA blots also revealed that each of these thymomas expressed two abnormal-size proviral transcripts detectable with the *ABL* kinase domain probe (Fig. 4B). In order to examine the structure of the proviral *BCR-ABL* coding region, *Eco*RI-digested genomic DNA was hybridized with the kinase domain probe as described in the legend to Fig. 2C. Each tumor was found to carry two *BCR-ABL* fragments (Fig. 4C). Two of the tumors shown in Fig. 4C (lanes 2 and 3) carried the expected 7.0-kb *BCR-ABL* proviral coding region as well as an aberrant-sized band, while the third tumor (Fig. 4C, lane 1) carried only two aberrant *BCR-ABL* bands. None of these tumors carried *neo*-hybridizing sequences (data not shown). The slight variation in hybridization intensity observed between the distinct *BCR-ABL* *Eco*RI restriction fragments present in individual tumors (Fig. 4C) suggests that each fragment is carried in separate tumor cell clones.

Thymic lymphomas arise from the transformation of few immature lymphoid cells. In order to determine whether the A-MuLV and *BCR-ABL* viruses induced tumors that arose from single or multiple independently transformed cells, DNA from several different thymomas was digested with restriction enzymes that cut in flanking genomic sequences and then hybridized with virus-specific probes. The data in Fig. 5 show that most A-MuLV/M- and P210/M-induced tumors contained one or two predominant proviral integrations, indicating that the tumors were primarily clonal in origin. The appearance of submolar hybridizing bands indicates that minor transformed populations were also present in some tumors. One A-MuLV-induced tumor (Fig. 2B, lane 4) carried two proviral bands which hybridized with equal intensity to each other and to the c-*abl* germ line band, suggesting that a single tumor clone may carry two proviral integrants. The absence of a proviral band in the P210/M-injected tumor shown in Fig. 5A (lane 7) was confirmed by hybridization of an *Eco*RI-digested genomic DNA blot with the kinase domain probe (data not shown), making it likely that this represents an Mo-MuLV-induced tumor. Unlike replication-defective viruses, Mo-MuLV usually integrates several times in infected cells, making it difficult to analyze Mo-MuLV tumor clonality by proviral integration. For this reason, the clonality of Mo-MuLV-induced tumors was analyzed by DNA blot analysis of the structures of the *IgH* and *TCR* genes. The data in Fig. 6A show clonal rearrangement patterns for these genes in most tumors, which indicates that Mo-MuLV tumors developed primarily from the malignant proliferation of a single thymocyte.

In order to compare the stage of differentiation of primary thymomas induced with the different viruses, the structures of the *IgH* and *TCR* beta and gamma genes were examined on DNA blots. Thymomas induced with Mo-MuLV and P210/M usually showed extensive rearrangement (including deletions) of both *TCR* beta alleles (Fig. 6A and C). Since our probe detects the 3′ untranslated region of *Cβ1* and does not cross-hybridize with *Cβ2*, deletions in *Cβ1* are probably due to rearrangement of *Cβ2*. In contrast to this complex pattern of *TCR* gene rearrangement, the *IgH* genes in most P210/M- and Mo-MuLV-induced thymomas either were not rearranged or had only one allele rearranged. It was interesting that hybridization with the J_H probe of Mo-MuLV tumor DNA digested with either *Eco*RI (Fig. 6A) or *Bam*HI and *Eco*RV (data not shown) showed that tumors with *IgH* rearrangements had a common rearranged band that was consistently smaller than the germ line band. From the

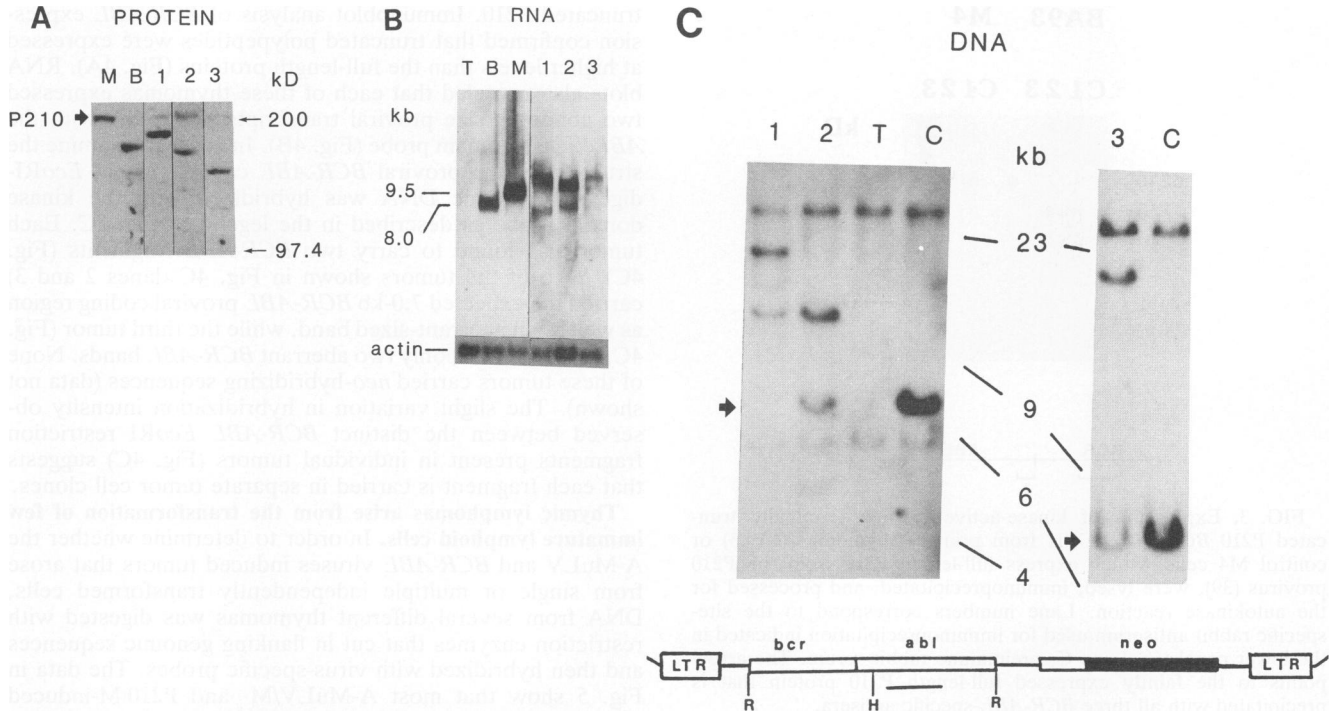

FIG. 4. Simultaneous expression of full-length and truncated P210 in tumors BA5.3, BA9.3, and BA10.1 (lanes 1 to 3, respectively). (A) Immunoblot analysis of *BCR-ABL* expression was done as described in the legend to Fig. 2, and ABL proteins were detected with a monoclonal antibody directed to the kinase domain. (B) RNA analysis of the same tumors as in panel A. Total RNA was analyzed as described in the legend to Fig. 2 and hybridized with a kinase domain probe. Lane M, M4 cells (pre-B cells that express P210); lane B, 78B4 cells (pre-B cells that express P185); lane T, uninfected thymus cells. (C) The structure of the integrated proviral genomes was examined by DNA blotting of *Eco*RI-digested tumor DNA as described in the legend to Fig. 2C. The 27-kb germ line band is seen in all lanes, and arrows point to the "wild-type" 7.0-kb *BCR-ABL* proviral DNA sequence. Lane C, P210/M-transformed pre-B-cell line that expresses only full-length P210. R, *Eco*RI; H, *Hin*dIII.

recurrence and reduced size of this band (2, 22), it may represent identical D_H-J_H rearrangements in independent tumors.

Unlike the thymic lymphomas induced with Mo-MuLV and the *BCR-ABL* virus, those induced with A-MuLV/M often maintained at least one germ line *IgH* and *TCR*β allele (Fig. 6B). For this reason, it is difficult to unambiguously assign tumor cells in these thymomas to either the T or B lineage on the basis of gene configuration alone.

***BCR-ABL* and v-*abl* viruses induce thymic lymphomas with different phenotypes.** To further investigate the phenotype of thymic lymphomas induced with the different viruses, expression of lineage and differentiation-restricted surface antigens was examined by flow cytometry. As expected, cells in Mo-MuLV-induced thymomas were almost entirely Thy-1$^+$ B220$^-$ T lymphocytes (Table 2). Tumors induced with A-MuLV/M and *BCR-ABL* virus were also largely Thy-1$^+$ T-lymphoid cells (Table 2), but in distinct contrast to Mo-MuLV thymomas, they often contained significant numbers (20 to 80%) of cells that expressed the B220 antigen normally found on B-lymphoid cells (Fig. 7 and Table 2). In some tumors, the simultaneous presence of B220$^+$ and Thy-1$^+$ cells suggests that separate thymocyte populations were transformed by the injected virus; however, in other tumors the sum of the percentage of B220$^+$ cells plus the percentage of Thy-1$^+$ cells was greater than 100% (Table 2, asterisks), which signifies the presence of cells that expressed B220 and Thy-1 simultaneously. B220$^+$ tumor cells did not express surface immunoglobulin, as determined by immunofluorescent staining, and maintained the immunoglobulin kappa gene in the germ line configuration (4), which rules out possible contamination by mature B lymphocytes from the circulation or from parathymic lymph nodes.

All tumors analyzed could be divided into four groups by CD4 and CD8 expression. Representative two-color histograms for each group are shown in Fig. 8. Cells from all Mo-MuLV-induced tumors contained CD4$^+$ CD8$^+$ cells (Fig. 8A and Table 2A), and some also contained a distinct CD4$^+$ CD8$^-$ population (Fig. 8B and Table 2B), which could represent a second transformed cell population in the tumor. Most of these tumors were also predominantly CD3$^-$ or CD3^{lo}, although a few tumors contained cells expressing CD3^{hi} (Table 2). Together, these data indicate that Mo-MuLV thymomas consist of cells in the early to intermediate stages of T-cell development.

Most thymomas induced with either v-*abl* or *BCR-ABL* oncogenes consisted primarily of CD8$^+$ cells that expressed a continuum of CD4 ranging from negative to positive (Fig. 8C and Table 2C), a phenotype that was not observed in any Mo-MuLV tumor examined. While *ABL* oncogene-induced tumors largely contained CD3$^-$ or CD3^{lo} cells (Table 2), representing an immature phenotype, CD3-expressing thymic T cells were more commonly found in *BCR-ABL* thymomas (Fig. 9 and Table 2). The reason that most cells were CD3$^-$ in some A-MuLV-induced thymomas could be the comparatively high numbers of Thy-1$^-$ B220$^+$ cells; however, other A-MuLV tumors with few B220$^+$ cells remained almost entirely CD3$^-$ (Table 2, tumors 15.3, 15.7, and 15.8).

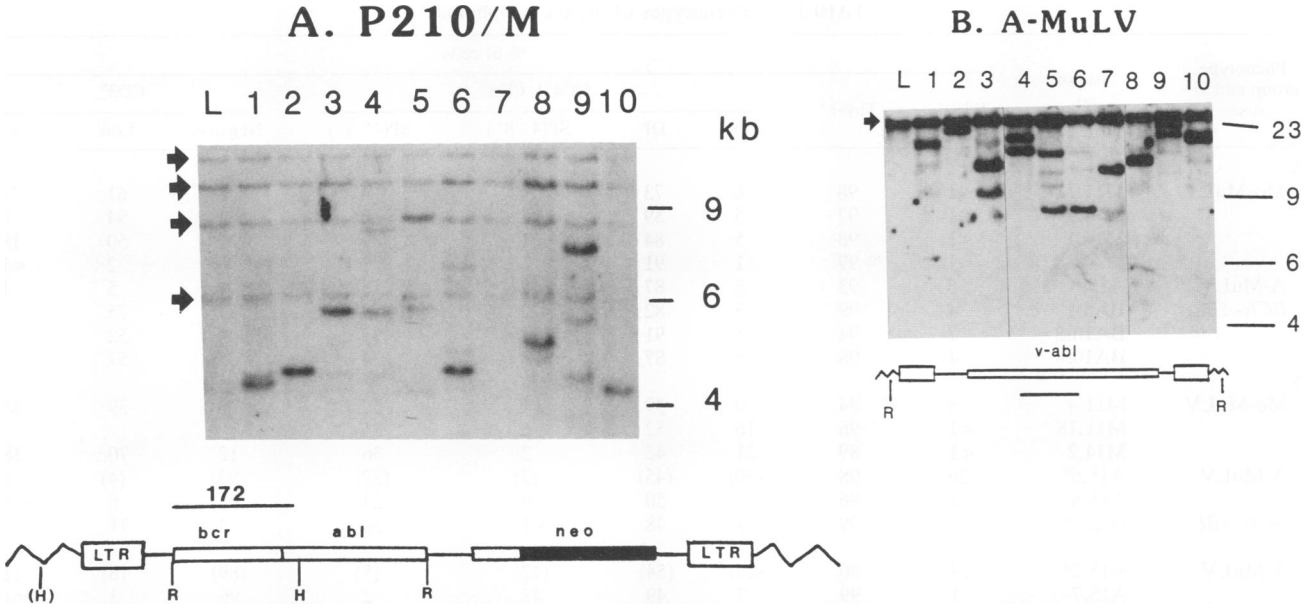

FIG. 5. Proviral integration. High-molecular-weight DNA (7.5 μg per lane) from P210/M-induced thymomas was digested with *Hin*dIII (H), which cuts once in the *ABL* sequence of the provirus and in 5′-flanking genomic DNA, depending on the site of integration. DNA from A-MuLV/M tumors was digested with *Eco*RI (R), which only cuts in flanking genomic DNA. Blots were hybridized with either the 172 cDNA probe, which recognizes 5′ *BCR* sequences as well as some *ABL* sequences just downstream of the *BCR-ABL* junction (A), or with a fragment from pAB3SUB3 (B). Arrows point to mouse germ line sequences detected with the probes. Lane L, uninfected liver cells (control).

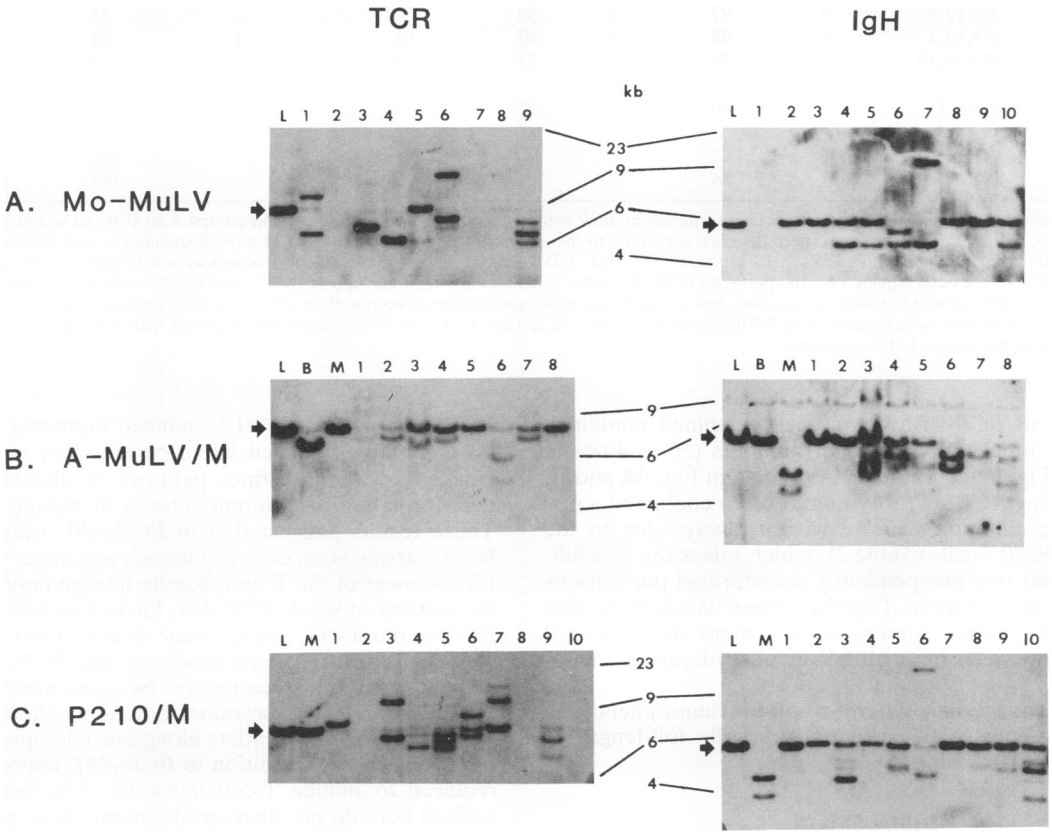

FIG. 6. Immunoglobulin and *TCR* gene structure of primary thymomas induced with different viruses. High-molecular-weight DNA from individual tumors was digested with *Eco*RI (for *IgH*) or with *Hin*dIII (for *TCR*) and probed with a J_H or Cβ1 probe, respectively. Lane L, normal liver cells (control); lane B, 78B4 cells (P185/M-transformed pre-B cells); lane M, M4 cells (P210/M-transformed pre-B cells). Arrows point to unrearranged germ line bands.

TABLE 2. Phenotypes of thymic lymphomas[a]

Phenotype group and viruses	Tumor no.	% of cells								
		B220$^+$	Thy-1$^+$	CD4 + CD8				CD3[b]		
				DN	DP	SP(4$^-$ 8$^+$)	SP(4$^+$ 8$^-$)	Negative	Low	High
A										
Mo-MuLV	M11.11	<1	98	6	73	14	6	8	61	31
	M11.19	<1	97	5	89	<1	6	<1	94	6
	M14.1	<1	98	5	84	1	9	32	50	18
	M14.3	<1	99	1	91	8	<1	98	2	<1
A-MuLV	A15.3	5	93	6	87	2	5	94	5	1
BCR-ABL	BA5.1	4	99	3	82	12	3	17	75	8
	BA10.2	7	94	5	91	2	2	44	52	4
	BA10.4	4	98	5	87	5	4	35	57	8
B										
Mo-MuLV	M11.4	8	94	9	39	1	50	16	39	45
	M11.18	<1	96	16	52	6	26			
	M14.2	<1	89	21	42	2	36	12	70	18
A-MuLV	A15.6*	26	98	(30)	(45)	(2)	(22)	(93)	(4)	(3)
	A15.8	1	96	16	50	9	24	93	6	<1
BCR-ABL	BA5.2	2	99	1	48	<1	50	3	71	26
C										
A-MuLV	A15.2*	24	90	(27)	(54)	(12)	(5)	(89)	(8)	(3)
	A15.7	1	99	7	49	42	2	96	3	<1
BCR-ABL[c]	BA7.1	8	96	5	70	23	2	43	38	19
	BA7.2	27	88	(25)	(30)	(35)	(10)	(38)	(53)	(9)
	BA9.3*	27	99	(35)	(23)	(30)	(12)	(57)	(37)	(7)
	BA9.4	8	96	19	50	23	7	78	13	9
	BA9.7	7	67	7	66	23	4	38	39	12
	BA9.11*	35	82	(30)	(38)	(20)	(11)	(45)	(17)	(39)
	BA10.1	6	99	3	69	26	2	63	33	5
	BA12.1	31	80	(33)	(29)	(32)	(5)	(82)	(17)	(1)
	BA12.5	4	97	8	58	30	4	34	64	2
	BA16.4	5	98	9	22	68	1	34	57	9
	BA16.16	6	78	27	31	34	8	14	57	30
D										
BCR-ABL	BA5.3	16	90	(20)	(10)	(58)	(9)	(79)	(19)	(3)
Other[d]										
A-MuLV	A15.1*	77	67					(88)	(7)	(5)
	A15.5	54	56					(88)	(11)	(<1)

[a] Immunophenotypes of thymic lymphomas were determined by flow cytometry, and tumors were placed in groups A to D by CD4 and CD8 phenotype as shown in Fig. 8. CD4 and CD8 phenotypes were assigned according to the quadrants identified by analysis of normal splenocyte and thymocyte controls. The values for normal thymocytes were 3.6% DN, 78.7% DP, 5.0% SP (CD4$^-$ CD8$^+$), and 12.8% SP (CD4$^+$ CD8$^-$). Numbers in parentheses represent the percentage of total cells and have not been adjusted for the presence of B220$^+$ cells. *, tumors in which the sum of B220$^+$ and Thy-1$^+$ cells was >100%.

[b] The scoring of CD3 staining intensity as negative, low, or high was based on staining of normal thymocytes for each analysis (Fig. 9).

[c] All *BCR-ABL* thymomas were induced with P210/M except for mice 12.1, 12.5, 16.4, and 16.16, which were injected with P185/M.

[d] CD4-CD8 T-cell phenotype not determined.

In contrast, all *BCR-ABL* thymomas examined contained CD3$^+$ cells, often with significant numbers (20 to 40%) of CD3^{hi} cells (Fig. 9 and Table 2). As shown in Fig. 9A and B, CD3-expressing *BCR-ABL* thymomas often contained a distinct CD3$^-$ population which was not always due to the presence of B220$^+$ cells (Table 2), which raises the possibility that at least two independently transformed populations were present in the tumor. Together, these data suggest that *BCR-ABL* can induce tumors with a more differentiated phenotype than seen in A-MuLV-induced thymic lymphomas.

There were no obvious differences in the tumor phenotype between thymomas that expressed primarily full-length or truncated *BCR-ABL* kinase.

DISCUSSION

This report demonstrates that *BCR-ABL* oncogenes can efficiently induce clonal or oligoclonal thymic lymphomas involving immature thymic lymphocytes. Although both *BCR-ABL*- and Mo-MuLV-induced thymomas appeared after a similar prolonged latent period, they could be distinguished by their distinct patterns of disease and by the transformation of different subsets of thymic lymphocytes. These results suggest that in *BCR-ABL* transformation of bone marrow stem cells of humans and mice, the infrequent involvement of the T-lymphocyte lineage may not be due to an inability of weak *BCR-ABL* kinases to transform T cells. Rather, the T-cell lineage may diverge from bone marrow stem cells prior to expression of the *BCR-ABL* gene by chromosome translocation or by gene transfer. Alternatively, *BCR-ABL* expression may affect the ability of progenitor cells to differentiate along the T-lymphocyte lineage. Finally, factors in addition to *BCR-ABL* expression may be required to induce T-cell leukemia. The experiments described here do not distinguish among these possibilities.

Phenotypes of thymic lymphomas. The presence of B220$^+$ cells clearly distinguished *BCR-ABL*- and v-*abl*-induced thymic lymphomas from tumors caused by Mo-MuLV. B220 is normally expressed on B lymphocytes and on hematolym-

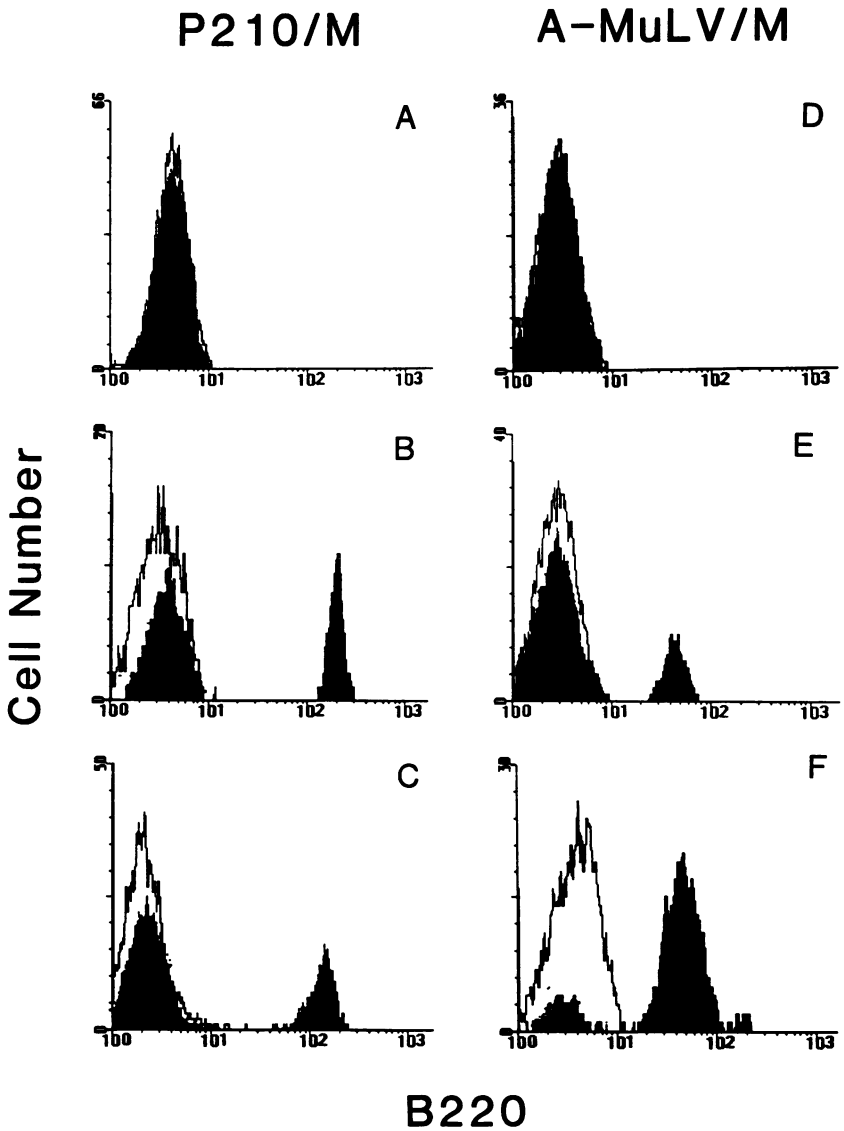

FIG. 7. Representative immunofluorescent detection of different levels of B220 expression in thymomas induced with P210/M and A-MuLV/M. Data for tumors BA5.2, BA7.2, and BA9.11 are presented in panels A to C, respectively, and for tumors A15.8, A15.1, and A15.2 are presented in panels D to F, respectively. Cells were stained with FITC-conjugated anti-B220 antibodies (solid histogram) or with FITC-conjugated isotype control antibody (open histogram) and analyzed by flow cytometry. Less than 0.5% of normal thymocytes stain positively for B220 (4).

phoid progenitor cells committed to the B lineage. The fact that $B220^+$ transformants were repeatedly found in v-*abl*- and *BCR-ABL*-induced thymic lymphomas suggests that a normal $B220^+$ cell resides in the thymus and may represent a highly preferred transformation target for *ABL*-expressing retroviruses. Other groups have isolated $B220^+$ Thy-1^- pre-B-lymphoid cells from v-*abl*- and v-*myc*-transformed thymi (3, 12, 50, 56), raising the possibility that the $B220^+$ cells that we observed in primary thymomas also represent pre-B-cell transformants. However, recent observations have shown that our $B220^+$ thymic transformants are also Thy-1^{lo} (4), which distinguishes them from other published $B220^+$ Thy-1^- cell lines. Less than 0.5% of normal thymocytes coexpress B220 and Thy-1^{lo} (4), similar to the phenotype of the bone marrow B-lymphocyte progenitor cell which is a preferred target for A-MuLV transformation (60). It is therefore possible that B-lymphocyte progenitors reside in the thymus and are transformed by *ABL* viruses. Experiments are under way to clarify the nature and origin of these rare $B220^+$ Thy-1^{lo} thymic lymphocytes.

All Mo-MuLV-induced thymomas consisted of $CD4^+$ cells that were either $CD8^+$ or $CD8^-$. The immature $CD4^+$ $CD8^+$ double-positive (DP) thymocyte population has been shown to give rise to mature $CD4^+$ $CD8^-$ T cells before giving rise to mature $CD4^-$ $CD8^+$ cells (46), which could account for the simultaneous appearance in some Mo-MuLV tumors of DP and $CD4^+$ single-positive (SP) cells in the absence of $CD8^+$ SP cells. However, because $CD4^+$ $CD8^+$ cells can arise from either $CD4^-$ $CD8^-$ double-negative (DN) precursors or from earlier $CD4^+$ or $CD8^+$ SP transitional stages (46), it is difficult to precisely determine the relationship between the DP and $CD4^+$ SP cells in Mo-MuLV tumors.

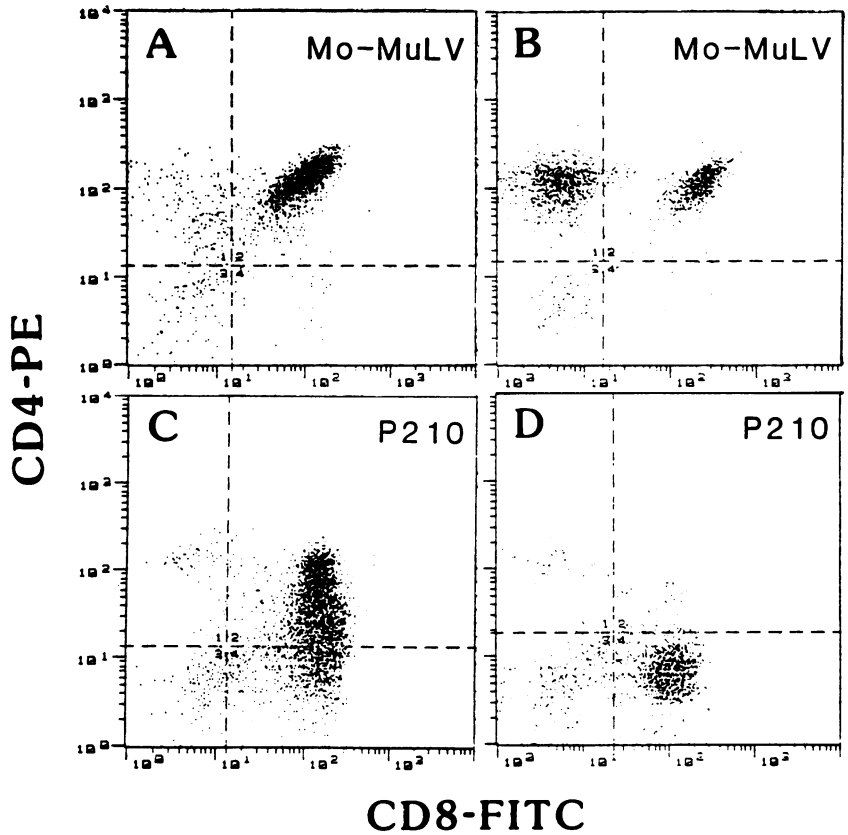

FIG. 8. Two-color immunofluorescent plots of CD4 and CD8 expression, showing representative phenotypes of primary thymomas. Gates were set according to isotype control staining and compared with CD4 and CD8 profiles of normal thymocytes. PE, phycoerythrin.

Finally, we cannot rule out the possibility that the presence of distinct phenotypic populations in the same tumor could result from more than one transformation event.

In distinct contrast to Mo-MuLV-induced tumors, individual v-*abl* and *BCR-ABL* thymomas consisted primarily of $CD8^+$ SP cells with a continuum of CD4 expression from negative to positive. Mice transgenic for the human *Ttg-1* oncogene also developed thymic lymphoma with this phenotype (38), which was concluded to represent a developmental stage in which early transitional $CD8^+$ cells give rise to $CD4^+$ $CD8^+$ progenitors (26, 43). However, given the fact that 20 to 40% of the cells in the *BCR-ABL*-induced but not in the v-*abl*-induced tumors expressed high levels of CD3, we cannot rule out that the phenotype of these tumors may represent a later transition stage in which $CD4^+$ $CD8^+$ progenitors develop into mature $CD8^+$ SP cells. If true, this raises the possibility that *BCR-ABL* may selectively stimulate the growth of an immature $CD4^+$ $CD8^+$ thymocyte population committed to the $CD8^+$ lineage, which could be useful for studying this important window of T-cell differentiation.

Consistent with the fact that A-MuLV usually transforms marrow-derived pre-B-lymphocytes that do not express surface antigen receptors (52), A-MuLV also transformed Thy-1^+ thymocytes that expressed minimal levels of the CD3-TCR complex. Conversely, in most *BCR-ABL*-induced tumors, greater than 40% of the cells expressed low to high levels of CD3. This is consistent with the possibility that *BCR-ABL* thymomas were more differentiated than v-*abl* thymomas. The A-MuLV and *BCR-ABL* viruses have been reported to cause slightly different types of leukemia in a hematopoietic stem cell transformation model (57), while P210 and P185 viruses transformed a similar spectrum of hematopoietic cell types (34). Either v-*abl* and *BCR-ABL* preferentially transform a different range of hematopoietic targets, or the different *ABL* kinases exert dissimilar effects on the maturation of infected hematolymphoid progenitor cells, resulting in malignancies with slightly different phenotypes. Finally, since Mo-MuLV tumors were usually $CD3^+$, it is possible that the population of $CD3^+$ cells in *BCR-ABL* thymomas reflects the presence of Mo-MuLV transformants.

Role of the helper virus. Although the data presented here demonstrate a role for *BCR-ABL* in the induction of thymic lymphoma in mice injected intrathymically with the P210/M or P185/M virus, we cannot exclude a possible effect of the Mo-MuLV helper virus in the pathogenesis of these tumors. Helper virus has been reported to be important for A-MuLV induction of pre-B lymphomas (48, 51, 53) but not for A-MuLV-induced thymomagenesis (47). It is therefore possible that thymocyte transformation by *BCR-ABL* viruses may not be affected by the helper virus. However, because *BCR-ABL* kinases are much less oncogenic than the v-*abl* kinase, it remains possible that a leukemogenic MuLV could influence the pathogenesis of *BCR-ABL*-induced thymic lymphoma. Mo-MuLV could affect *BCR-ABL* thymomagenesis either by facilitating the spread of the defective *BCR-ABL* virus to rare transformable thymic target cells or by functioning as an insertional mutagen (14, 58, 61), disrupting the expression of cellular proto-oncogenes capable of coop-

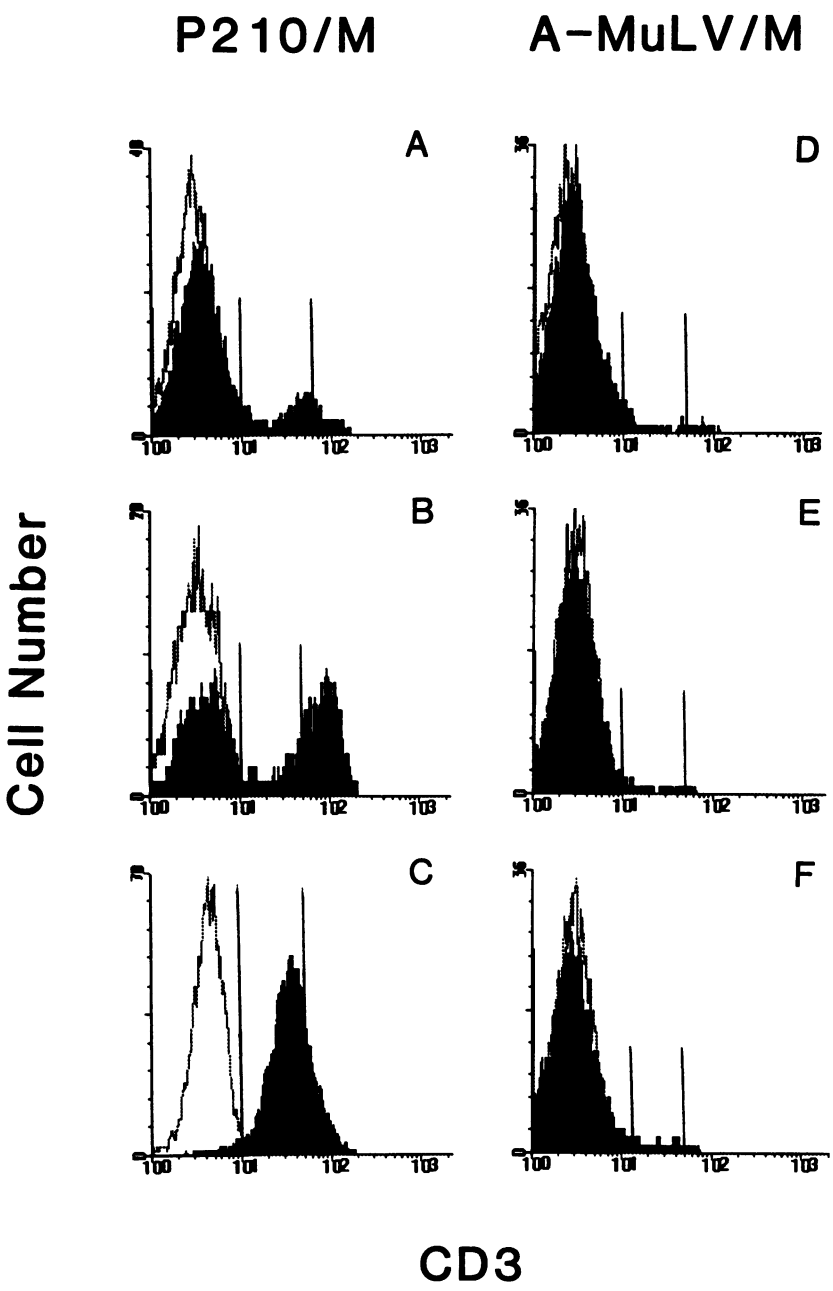

FIG. 9. Representative immunofluorescent staining showing variable levels of CD3 expression in P210/M thymomas and negligible expression in A-MuLV/M-induced tumors. (A, B, and C) P210/M-induced thymomas BA9.4, BA9.11, and BA5.2, respectively; (D, E, and F) A-MuLV/M-induced tumors A15.3, A15.7, and A15.8, respectively. Cursors are drawn to show $CD3^-$, $CD3^{lo}$, and $CD3^{hi}$ limits determined for each analysis by staining normal thymi.

erating with *BCR-ABL* kinases. Oncogenic cooperation between the *BCR-ABL* and *MYC* oncogenes has been shown in lymphocyte and fibroblast transformation models (37, 54).

The presence of the Mo-MuLV helper virus could also affect the presentation of thymic lymphomas induced with a *BCR-ABL*/Mo-MuLV virus through independent transformation of separate thymocyte populations by Mo-MuLV and *BCR-ABL* viruses. Such an effect could feasibly explain several of the observations reported here, including the appearance of both Mo-MuLV and P210 patterns of disease in P185/M-induced thymomas, low and variable *BCR-ABL* oncogene expression, and phenotypic heterogeneity in some tumors. However, the fact that we found a fairly consistent level of *BCR-ABL* proviral DNA in thymic tumors from different animals indicates either that a putative Mo-MuLV-transformed population was equally represented in each tumor or that transformation by Mo-MuLV contributed little to the phenotype and presentation of *BCR-ABL*-induced thymic tumors. The latter possibility is compatible with the observation that tumors induced by intrathymic injection of Mo-MuLV alone showed predominantly extrathymic involvement. Thus, Mo-MuLV-transformed cells, if present,

might not markedly influence the presentation of *BCR-ABL* tumors, which characteristically display more significant thymic involvement.

Initial attempts have been made to circumvent the helper virus by intrathymic injection of a helper-free P210 *BCR-ABL* virus, but these experiments have been hindered by the low titer of the virus. Still, the one animal (out of ten injected) which did develop a tumor showed massive thymic lymphoma with very little peripheral disease (7), which is identical to the pathology seen in mice injected with P210/M. These preliminary data indicate that helper virus is not absolutely necessary for *BCR-ABL*-induced thymomagenesis. It should be possible to avoid the virus titer problem by using *BCR-ABL* virus pseudotyped with nonleukemogenic MuLV or by using other strategies to develop higher-titer helper-free virus (7, 42).

Oncogene expression in primary thymomas. In contrast to the consistently high level of v-*abl* expression in A-MuLV tumors, *BCR-ABL* expression was more variable. While this could be due to the presence in the tumor population of Mo-MuLV transformants which do not express *BCR-ABL*, heterogeneous *BCR-ABL* protein expression correlated with proviral RNA levels, while the proviral DNA level was found to be relatively constant between tumors. Together, these observations indicate that inconsistent oncogene expression was controlled, at least in part, at the RNA level rather than by variability in infection efficiency. Transcriptional heterogeneity could result from a positional effect of the site of proviral DNA integration; however, a similar positional effect should also affect v-*abl* expression, which was not seen. It seems more likely that the stability of *BCR-ABL* transcripts was affected by recombination in the *BCR-ABL* provirus that may have resulted in loss of the 3′ LTR. Similar proviral recombination in A-MuLV/M-transformed thymi or in other *BCR-ABL*-transformed hematopoietic cells has not been seen, but multiple rounds of virus replication may be required for retrovirus variants to arise, and this might occur more efficiently in vivo (44), especially during the significantly longer latent period required for the development of *BCR-ABL* tumors than for v-*abl* tumors. The instability of *BCR-ABL* retroviruses could also relate to the relatively large size (approximately 10 kb) of the viral genome.

Several independent tumors induced with *BCR-ABL* virus expressed C-terminally truncated P210 or P185 kinase-active products. Since oncogene truncation has not been observed in *BCR-ABL*-transformed B-lymphoid cells or in v-*abl*-induced thymomas, this could point to a distinct effect of *BCR-ABL* on developing T lymphocytes. The determinants for the diverse effects of *ABL* kinase activity on different cell lineages have, in fact, been mapped to the C terminus; these effects include a cytotoxic effect in fibroblasts (16, 66) and reduced transformation efficiency in B-lymphoid cells (44, 49, 63). Still, it remains possible that the appearance of tumors expressing C-terminally truncated *BCR-ABL* oncoproteins may not be due to a special effect of the *BCR-ABL* kinase on T cells. In all rearranged proviruses examined, including those in which the *BCR-ABL* coding region was not appreciably affected, the proviral *neo* sequences were consistently deleted. Thus, transformed T cells which express *neo* could have a growth disadvantage compared with transformants that do not express *neo*. Expression of *neo* has been shown to delay differentiation of HL-60 human promyelocytic leukemia cells (62) and to increase glucocorticoid toxicity in a human T-cell line (15). The data presented here are not sufficient for determining whether deletion of downstream *BCR-ABL* sequences, loss of *neo* expression, or both affect the growth of transformed thymocytes.

In conclusion, these studies demonstrate that weak *BCR-ABL* oncogenes can affect the early stages of T-lymphocyte development. Since *BCR-ABL* transformation provides a way to study the dynamic processes that regulate B-cell lymphopoiesis (55), a similar thymocyte transformation model may be useful for studying the regulation of T-cell development.

ACKNOWLEDGMENTS

We thank Monica Woldt, Ann Krueger, and John Kelly for technical assistance; Larry Morrissey for flow cytometry analysis; and Richard Schwartz, Rex Risser, and Fred Blattner for molecular probes. S.S.C. is especially grateful for the support and friendship provided by Rex Risser (deceased) during the early stages of this work.

This work was supported in part by awards to S.S.C. from the James D. and Dorothy Shaw Fund in the Milwaukee Foundation and by NIH grants CA52142 and CA14520 (Core), ACS institutional grant SIG15, and a generous gift to the UWCCC from Mr. and Mrs. Donald Anderson. O.N.W. is an Investigator of the Howard Hughes Medical Institute.

REFERENCES

1. **Andrews, D. F., and S. J. Collins.** 1987. Heterogeneity in expression of the bcr-abl fusion transcript in CML blast crisis. Leukemia **1**:718–24.
2. **Born, W., J. Yague, E. Palmer, J. Kappler, and P. Marrack.** 1985. Rearrangement of T cell receptor beta chain genes during T cell development. Proc. Natl. Acad. Sci. USA **82**:2925–2929.
3. **Brightman, B. K., K. G. Chandy, R. H. Spencer, S. Gupta, P. K. Pattengale, and H. Fan.** 1988. Characterization of lymphoid tumors induced by a recombinant murine retrovirus carrying the avian v-myc oncogene. J. Immunol. **141**:2844–2854.
4. **Chen, E., B. Swanson, and S. S. Clark.** Unpublished data.
5. **Clark, S., J. McLaughlin, W. Crist, R. Champlin, and O. Witte.** 1987. Unique forms of the abl tyrosine distinguish Ph-positive CML from Ph-positive ALL. Science **235**:85–88.
6. **Clark, S., J. McLaughlin, M. Timmons, A. M. Pendergast, L. Dow, W. Crist, G. Rovera, S. D. Smith, and O. N. Witte.** 1988. Expression of a distinctive bcr-abl oncogene in Ph-positive acute lymphocytic leukemia. Science **239**:775–777.
7. **Clark, S. S.** Unpublished data.
8. **Clark, S. S., W. M. Crist, R. Champlin, and O. N. Witte.** 1989. Molecular pathogenesis of bcr-abl oncogene expression in Ph^+ leukemias, p. 15–20. *In* M. Greaves (ed.), Molecular diagnosis of human leukemia. Cancer cells, vol. 7. Cold Spring Harbor Laboratory, Cold Spring Harbor, N.Y.
9. **Clark, S. S., W. M. Crist, and O. N. Witte.** 1989. Molecular pathogenesis of Ph-positive leukemias. Annu. Rev. Med. **40**: 113–122.
10. **Cook, W.** 1982. Rapid thymomas induced by Abelson murine leukemia virus. Proc. Natl. Acad. Sci. USA **79**:2917–2921.
11. **Cook, W.** 1985. Thymocyte subsets transformed by Abelson murine leukemia virus. Mol. Cell. Biol. **5**:390–397.
12. **Cook, W. D., and A. M. Balaton.** 1987. T-cell receptor and immunoglobulin genes are rearranged together in Abelson virus-transformed pre-B or pre-T cells. Mol. Cell. Biol. **7**:266–272.
13. **Cook, W. D., D. Metcalf, N. Nicola, A. W. Burgess, and F. Walker.** 1985. Malignant transformation of a growth factor dependent myeloid cell line by Abelson virus without evidence of an autocrine mechanism. Cell **41**:677–683.
14. **Corcoran, L., J. Adams, A. Dunn, and S. Cory.** 1984. Murine T lymphomas in which the cellular myc oncogene has been activated by retrovirus insertion. Cell **37**:113–122.
15. **de Cuevillas, F., and H. Lachman.** 1990. Transfection of a T-cell line with neo increases dexamethasone cytotoxicity. Leukemia Res. **14**:623–627.
16. **Daley, G., J. McLaughlin, O. Witte, and D. Baltimore.** 1987. The CML-specific P210 bcr/abl protein, unlike v-abl, does not trans-

form NIH/3T3 fibroblasts. Science 237:532–535.
17. **Daley, G. Q., R. Van Etten, and D. Baltimore.** 1990. Induction of chronic myelogenous leukemia in mice by the P210 bcr/abl gene of the Philadelphia chromosome. Science 247:824–830.
18. **Denis, K., L. Treiman, J. St. Claire, and O. Witte.** 1984. Long term cultures of murine fetal liver retain very early B lymphoid phenotype. J. Exp. Med. 160:1087–1101.
19. **Dreazen, O., E. Canaani, and R. P. Gale.** 1988. Molecular biology of chronic myelogenous leukemia. Semin. Hematol. 25:35–49.
20. **Elefanty, A. G., and S. Cory.** 1992. Hematologic disease induced in BALB/c mice by a *bcr-abl* retrovirus is influenced by the infection conditions. Mol. Cell. Biol. 12:1755–1763.
21. **Elefanty, A. G., I. K. Hariharan, and S. Cory.** 1990. bcr-abl, the hallmark of chronic myelogenous leukemia in man, induces multiple haematopoietic neoplasms in mice. EMBO J. 9:1069–1078.
22. **Forster, A., S. Huck, N. Ghanem, M.-P. Lefranc, and T. H. Rabbitts.** 1987. New subgroups in the human T cell rearranging V-gamma gene locus. EMBO J. 6:1945–1950.
23. **Gishizky, M., J. McLaughlin, and O. N. Witte.** 1991. The 5′ noncoding region of the BCR/ABL oncogene augments its ability to stimulate the growth of immature lymphoid cells. Oncogene 8:1299–1306.
24. **Gishizky, M., and O. N. Witte.** 1992. Initiation of deregulated growth of multipotential progenitor cells by bcr-abl in vitro. Science 256:836–839.
25. **Goff, S. P., C. J. Tabin, J. Y. J. Wang, R. Weinberg, and D. Baltimore.** 1982. Transfection of fibroblasts by cloned Abelson murine leukemia virus DNA and recovery of transmissable virus by recombination with helper virus. J. Virol. 41:271–285.
26. **Guidos, C. J., I. L. Weissman, and B. Adkins.** 1989. Intrathymic maturation of murine T lymphocytes from $CD8^+$ precursors. Proc. Natl. Acad. Sci. USA 86:7542–7546.
27. **Hariharan, I. K., A. W. Harris, M. Crawford, H. Abud, E. Webb, S. Cory, and J. A. Adams.** 1989. A *bcr-abl* oncogene induces lymphomas in transgenic mice. Mol. Cell. Biol. 9:2798–2805.
28. **Hedrick, S. M., E. A. Nielsen, J. Kavaler, D. I. Cohen, and M. M. Davis.** 1984. Isolation of cDNA clones encoding T cell-specific membrane-associated proteins. Nature (London) 308:153–158.
29. **Heisterkamp, N., G. Jenster, J. TenHoeve, D. Zovich, P. K. Pattengale, and J. Groffen.** 1990. Acute leukemia in bcr/abl transgenic mice. Nature (London) 344:251–253.
30. **Henderson, A., and K. Dorshkind.** 1990. In vitro models of B lymphocyte development. Semin. Immunol. 2:181–187.
31. **Holland, G., K. Ito, D. Kaehler, S. Tonegawa, and R. Risser.** 1991. Thymic targets for Abelson murine leukemia virus are early gamma-delta T lymphocytes. Proc. Natl. Acad. Sci. USA 88:3700–3704.
32. **Ito, K., M. Bonneville, Y. Takagaki, N. Nakanishi, O. Kanagawa, and S. Tonegawa.** 1989. Different gamma-delta T-cell receptors are expressed on thymocytes ad different stages of development. Proc. Natl. Acad. Sci. USA 86:631–635.
33. **Jonas, D., M. Lubbert, E. Kawasaki, M. Henke, K. Bross, R. Metelsmann, and F. Herrmann.** 1992. Clonal analysis of bcr-abl rearrangement in T lymphocytes from patients with chronic myelogenous leukemia. Blood 79:1017–1023.
34. **Kelliher, M., A. Knott, J. McLaughlin, O. N. Witte, and N. Rosenberg.** 1991. Differences in oncogenic potency but not target cell specificity distinguish the two forms of the *BCR/ABL* oncogene. Mol. Cell. Biol. 11:4710–4716.
35. **Kelliher, M., J. McLaughlin, O. N. Witte, and N. Rosenberg.** 1990. Induction of a chronic myelogenous-like syndrome in mice with v-abl and BCR/ABL. Proc. Natl. Acad. Sci. USA 87:6649–6653.
36. **Konopka, J. B., S. S. Clark, J. McLaughlin, M. Nitta, Y. Kato, A. Strife, B. Clarkson, and O. Witte.** 1986. Variable expression of the translocated c-abl oncogene in Philadelphia chromosome-positive B-lymphoid cell lines from chronic myelogenous leukemia patients. Proc. Natl. Acad. Sci. USA 83:4049–4052.
37. **Lugo, T., and O. Witte.** 1989. The BCR-ABL oncogene transforms Rat-1 cells and cooperates with v-*myc*. Mol. Cell. Biol. 9:1263–1270.
38. **McGuire, E. A., C. E. Rintoul, G. M. Sclar, and S. J. Korsmeyer.** 1992. Thymic overexpression of *Ttg-1* in transgenic mice results in T-cell acute lymphoblastic leukemia/lymphoma. Mol. Cell. Biol. 12:4186–4196.
39. **McLaughlin, J., E. Chianese, and O. Witte.** 1987. In vitro transformation of immature hematopoietic cells by the P210 bcr/abl oncogene product of the Philadelphia chromosome. Proc. Natl. Acad. Sci. USA 84:6558–6562.
40. **McLaughlin, J., E. Chianese, and O. N. Witte.** 1989. Alternative forms of the *BCR/ABL* oncogene have quantitatively different potencies for stimulation of immature lymphoid cells. Mol. Cell. Biol. 9:1866–1874.
41. **Mes-Masson, A. M., J. McLaughlin, G. Q. Daley, M. Paskind, and O. Witte.** 1986. Overlapping cDNA clones define the complete coding region for the P210 gene product associated with chronic myelogenous leukemia cells containing the Philadelphia chromosome. Proc. Natl. Acad. Sci. USA 83:9768–9772.
42. **Muller, A. J., J. C. Young, A. M. Pendergast, M. Pondel, N. R. Landau, D. R. Littman, and O. N. Witte.** 1991. *BCR* first exon sequences specifically activate the *BCR/ABL* tyrosine kinase oncogene of Philadelphia chromosome-positive human leukemias. Mol. Cell. Biol. 11:1785–1792.
43. **Nikolic-Zugic, J., and M. J. Bevan.** 1988. Thymocytes expressing CD8 differentiate into $CD4^+$ cells following intrathymic injection. Proc. Natl. Acad. Sci. USA 85:8633–8637.
44. **Parmar, K., R. C. Huebner, and N. Rosenberg.** 1991. Carboxyl-terminal determinants of Abelson protein important for lymphoma induction. J. Virol. 65:6478–6485.
45. **Paskind, M. P., R. A. Weinberg, and D. Baltimore.** 1975. Dependence of Moloney murine leukemia virus production on cell growth. Virology 67:242–248.
46. **Petrie, H. T., P. Hugo, R. Scollay, and K. Shortman.** 1990. Lineage relationships and developmental kinetics of immature thymocytes: CD3, CD4 and CD8 acquisition in vitro and in vivo. J. Exp. Med. 172:1583–1588.
47. **Poirier, Y., and P. Jolicoeur.** 1989. Distinct helper virus requirements for Abelson murine leukemia virus-induced pre-B- and T-cell lymphomas. J. Virol. 63:2088–2098.
48. **Poirier, Y., C. Kozak, and P. Jolicoeur.** 1988. Identification of a common helper provirus integration site in Abelson murine leukemia virus-induced lymphoma DNA. J. Virol. 62:3985–3992.
49. **Prywes, R., J. Foulkes, N. Rosenberg, and D. Baltimore.** 1983. Sequences of the A-MuLV protein needed for fibroblast and lymphoid cell transformation. Cell 34:569–579.
50. **Risser, R., D. Kaehler, and W. Lamph.** 1985. Different genes control susceptibility of mice to Moloney or Abelson murine leukemia viruses. J. Virol. 55:547–553.
51. **Rosenberg, N., and D. Baltimore.** 1978. The effect of helper virus on Abelson virus-induced transformation of lymphoid cells. J. Exp. Med. 147:1126–1141.
52. **Rosenberg, N., and O. Witte.** 1988. The viral and cellular forms of the Abelson (abl) oncogene. Adv. Virus Res. 35:39–81.
53. **Savard, P., L. DesGroseillers, E. Rassart, Y. Poirier, and P. Jolicoeur.** 1987. Important role of the long terminal repeat of the helper Moloney murine leukemia virus in Abelson virus-induced lymphoma. J. Virol. 61:3266–3275.
54. **Sawyers, C. L., W. Callahan, and O. N. Witte.** 1992. Dominant negative MYC blocs transformation by ABL oncogenes. Cell 70:901–910.
55. **Scherle, P., K. Dorshkind, and O. Witte.** 1990. Clonal lymphoid progenitor cell lines expressing the BCR/ABL oncogene retain full differentiative function. Proc. Natl. Acad. Sci. USA 87:1908–1912.
56. **Scott, M. L., M. M. Davis, and M. B. Feinberg.** 1986. Transformation of T-lymphoid cells by Abelson murine leukemia virus. J. Virol. 59:434–443.
57. **Scott, M. L., R. A. Van Etten, G. Daley, and D. Baltimore.** 1991. v-abl causes hematopoietic disease distinct from that caused by bcr-abl. Proc. Natl. Acad. Sci. USA 88:6506–6510.

58. **Selten, G., H. Cuypers, and A. Berns.** 1985. Proviral activation of the putative oncogene pim-1 in MuLV-induced T-cell lymphoma. EMBO J. **4**:1793–1798.
59. **Strife, A., and B. Clarkson.** 1988. Biology of chronic myelogenous leukemia: is discordant maturation the primary defect? Semin. Hematol. **25**:1–9.
60. **Tidmarsh, G., S. Heimfeld, C. Whitlock, I. L. Weissman, and C. E. Muller-Sieburg.** 1989. Identity of a novel bone marrow-derived B-cell progenitor population that coexpresses B220 and Thy-1 and is highly enriched for Abelson leukemia virus targets. Mol. Cell. Biol. **9**:2665–2671.
61. **van Lohuizen, M., M. Bouer, and A. Berns.** 1989. N-myc is frequently activated by proviral insertion in MuLV-induced T cell lymphoma. EMBO J. **8**:133–136.
62. **von Melcher, H., and D. E. Houseman.** 1988. The expression of neomycin phosphotransferase in human promyelocytic leukemia cells (HL60) delays their differentiation. Oncogene **2**:621–628.
63. **Watanabe, S., and O. Witte.** 1983. Site-directed deletions of Abelson murine leukemia virus define 3′ sequences essential for transformation and lethality. J. Virol. **45**:1028–1036.
64. **Whitlock, C., S. Ziegler, L. Treiman, J. Stafford, and O. N. Witte.** 1983. Differentiation of cloned populations of immature B cells after transformation with Abelson murine leukemia virus. Cell **32**:903–911.
65. **Ziegler, S., L. Treiman, and O. N. Witte.** 1984. Kappa gene diversity among the clonal progeny of pre-B lymphocytes. Proc. Natl. Acad. Sci. USA **81**:1529–1533.
66. **Ziegler, S., C. Whitlock, S. Goff, A. Gifford, and O. N. Witte.** 1981. Lethal effect of the Abelson murine leukemia virus transforming gene product. Cell **27**:477–486.